



## University of Dundee

Post-mortem AT-8 reactive tau species correlate with non-plaque A $\beta$  levels in the frontal cortex of non-AD and AD brains

Malik, Nauman; Miah, Mohi-Uddin; Galgani, Alessandro; McAleese, Kirsty E.; Walker, Lauren; LeBeau, Fiona E. N.

DOI:  
[10.1101/2023.09.27.559720](https://doi.org/10.1101/2023.09.27.559720)

Publication date:  
2023

Licence:  
CC BY

Document Version  
Early version, also known as pre-print

[Link to publication in Discovery Research Portal](#)

*Citation for published version (APA):*

Malik, N., Miah, M.-U., Galgani, A., McAleese, K. E., Walker, L., LeBeau, F. E. N., Attems, J., Outeiro, T. F., Thomas, A. J., & Koss, D. (2023). Post-mortem AT-8 reactive tau species correlate with non-plaque A $\beta$  levels in the frontal cortex of non-AD and AD brains. *BioRxiv*. <https://doi.org/10.1101/2023.09.27.559720>

**General rights**

Copyright and moral rights for the publications made accessible in Discovery Research Portal are retained by the authors and/or other copyright owners and it is a condition of accessing publications that users recognise and abide by the legal requirements associated with these rights.

**Take down policy**

If you believe that this document breaches copyright please contact us providing details, and we will remove access to the work immediately and investigate your claim.

1 **Post-mortem AT-8 reactive tau species correlate with non-**  
2 **plaque A $\beta$  levels in the frontal cortex of non-AD and AD**  
3 **brains**

4  
5 **Authors:**  $\S$ Nauman Malik<sup>1</sup>,  $\S$ Mohi-Uddin Miah<sup>1</sup>, Alessandro Galgani<sup>1</sup>, Kirsty McAleese<sup>1</sup>,  
6 Lauren Walker<sup>1</sup>, Fiona E. LeBeau<sup>2</sup>, Johannes Attems<sup>1</sup>, Tiago F. Outeiro<sup>1,3,4</sup>, Alan Thomas<sup>1</sup>,  
7 David J. Koss<sup>1+5\*</sup>

8  
9  $\S$ = these authors contributed equally.

- 10 1. Translational and Clinical Research Institute, Faculty of Medical Sciences, Newcastle  
11 University, UK.  
12 2. Biosciences, Faculty of Medical Sciences, Newcastle University, Newcastle-upon-  
13 Tyne, UK.  
14 3. Department of Experimental Neurodegeneration, Center for Biostructural Imaging of  
15 Neurodegeneration, University Medical Center Goettingen, Göttingen, Germany  
16 4. Max Planck Institute for Multidisciplinary Sciences, Göttingen, Germany  
17 5. Division of Cellular and Systems Medicine, School of Medicine, University of Dundee,  
18 Dundee.

19 \*Corresponding author= David J. Koss ([dkoss001@dundee.ac.uk](mailto:dkoss001@dundee.ac.uk)).  
20  
21  
22  
23  
24  
25  
26  
27

28 **Abstract**

29 The amyloid cascade hypothesis states that A $\beta$  and its aggregates induce pathological changes in tau,  
30 leading to formation of neurofibrillary tangles (NFTs) and cell death. A caveat with this hypothesis is  
31 the temporo-spatial divide between plaques and NFTs. This has been addressed by the inclusion of  
32 soluble species of A $\beta$  and tau in the revised amyloid cascade hypothesis, however, the demonstration  
33 of a correlative relationship between A $\beta$  and tau burden in post-mortem human tissue has remained  
34 elusive. Employing frozen and fixed frontal cortex grey and associated white matter tissue from non-  
35 AD controls (Con; n=39) and Alzheimer's diseases (AD) cases (n=21), biochemical and  
36 immunohistochemical measures of A $\beta$  and AT-8 phosphorylated tau were assessed. Native-state dot-  
37 blot from crude tissue lysates demonstrated robust correlations between intraregional A $\beta$  and AT-8  
38 tau, such increases in A $\beta$  immunoreactivity conferred increases in AT-8 immunoreactivity, both when  
39 considered across the entire cohort as well as separately in Con and AD cases. In contrast, no such  
40 association between A $\beta$  plaques and AT-8 were reported when using immunohistochemical  
41 measurements. However, when using the non-amyloid precursor protein cross reactive MOAB-2,  
42 antibody to measure intracellular A $\beta$  within a subset of cases, a similar correlative relationship with  
43 AT-8 tau as that observed in biochemical analysis was observed. Collectively our data suggests that  
44 accumulating intracellular A $\beta$  may influence AT-8 pathology. Despite the markedly lower levels of  
45 phospho-tau in non-AD controls correlative relationships between AT-8 phospho-tau and A $\beta$  as  
46 measured in both biochemical and immunohistochemical assays were more robust in non-AD  
47 controls, suggesting a physiological association of A $\beta$  production and tau phosphorylation, at least  
48 within the frontal cortex. Such interactions between regional A $\beta$  load and phospho-tau load may  
49 become modified with disease potentially, as a consequence of interregional tau seed propagation,  
50 and thus may diminish the linear relationship observed between A $\beta$  and phospho-tau in non-AD  
51 controls. This study provides evidence supportive of the revised amyloid cascade hypothesis, and  
52 demonstrates an associative relationship between AT-8 tau pathology and intracellular A $\beta$  but not  
53 extracellular A $\beta$  plaques.

54

55

56

57

58

59

## 60 Introduction

61 The original amyloid cascade hypothesis stated that the extracellular deposition of insoluble beta-  
62 amyloid (A $\beta$ ) plaques drives intracellular tau phosphorylation, the formation of neurofibrillary tangles  
63 (NFTs), and the subsequent neurodegeneration which underlies the pathology of Alzheimer's disease  
64 (AD) [1]. Owing to the lack of correlation between plaque burden and cognitive impairment, as well  
65 as a growing understanding of the toxicity of fibrillar and pre-fibrillar intermediate species, the  
66 hypothesis has been revised to include roles for A $\beta$  oligomers and tau oligomers[2]. Whilst the recent  
67 outcomes of plaque clearing and A $\beta$  oligomer targeted immunotherapies[3-5] support this revised  
68 amyloid cascade hypothesis, several inconsistencies relating to the interaction of A $\beta$  and tau remain.

69 Foremost, is the spatio-temporal disconnect between the emergence and progression of A $\beta$  plaque  
70 and tau NFT pathology. Based on the post-mortem neuropathological Thal phases of A $\beta$  deposition  
71 and positron emission tomography (PET) imaging studies A $\beta$  plaques originate within the neocortex,  
72 specifically within the orbito-frontal and medial parietal cortices, before spreading to the  
73 hippocampus, the brain stem and cerebellum[6, 7]. In contrast, as reflected by Braak NFT staging, tau  
74 pathology initially occurs in the entorhinal cortex and hippocampus and subsequently spreads to the  
75 lateral temporal and parietal cortices and finally to the frontal and occipital cortices[8, 9].

76 Cross sectional population studies further highlight the independent nature of the two hallmark  
77 pathologies, reporting that tau pathology consistent with Braak Stages I-II, occurs more readily with  
78 age than that of plaque depositions[10]. Consequently, A $\beta$  deposition is not a prerequisite for NFT  
79 formation in aging, nor in the cases of primary tauopathies[11]. The independence of tau pathology  
80 from A $\beta$  plaques is particularly evident in cases of primary age-related tauopathies (PART), which  
81 present with AD related NFTs in a spatial pattern consistent with Braak NFT stages up to stage IV  
82 without A $\beta$  plaque deposition[12]. Moreover, the demonstration of prion-like spreading via tau seed  
83 templating and pathology propagation, provides a mechanistic process by which the presence of tau  
84 pathology may occur independent from the influence of A $\beta$  plaques[13]. Such tau seed propagation  
85 of pathology likely contributes to the progression of tau pathology in many tauopathies, including AD.

86 Taken together, the direct causation of NFTs, purely as a consequence of A $\beta$  plaque burden is difficult  
87 to ratify, with the differential emergence in time and space of the neuropathological hallmarks, as well  
88 as the independent occurrence of tau aggregations in other neurodegenerative conditions.

89 However, it remains likely that plaque deposition or rather the process of amyloid plaque formation,  
90 influences the generation of tau pathology. This is perhaps most strongly supported by numerous  
91 biochemical studies of human brain tissue, which report robust correlations with pathological A $\beta$  and

92 tau species[14-17]. Despite the close relationship between tau and A $\beta$  levels in various biochemical  
93 assays, histochemical approaches frequently fail to detect such correlations. The disconnect between  
94 biochemical and histochemical analysis clearly highlights differences in the pathological species  
95 measured within the different methodological approaches.

96 In line with the revised amyloid cascade hypothesis[2], a range of experimental models demonstrate  
97 that soluble pathological species of both tau and A $\beta$  exert toxic influence within the brain, evident in  
98 injection models [18-21], familial AD (FAD) [22-24], tauopathy[25-27] mouse models and cell culture  
99 approaches[28, 29]. Whilst APP centric FAD mouse models, do not develop NFTs, there is clear  
100 evidence of increased tau phosphorylation within these models. Moreover in multi-genic mice, in  
101 which a human mutant tau gene is included, APP centric mutations can accelerate and enhance NFT  
102 pathology[30]. Nevertheless, evidence for the induction of tau pathology following A $\beta$  intracerebral  
103 delivery is sparse in non-transgenic animals[31, 32] and even in tau transgenic mice[33].

104 Whilst there are several possible explanations for the failure of exogenous A $\beta$  to drive tau pathology  
105 in-vivo, one possible contributing factor is that the sole delivery of A $\beta$  to the extracellular space may  
106 not be sufficient to drive tau pathology. Indeed, a growing body of evidence suggests that intracellular  
107 A $\beta$  accumulation may also play a role in the pathobiology of AD[34], influencing cellular  
108 dysfunction[35-37] and tau phosphorylation[22].

109 Despite the potential for non-plaque A $\beta$  to contribute to the production of tau pathology, few studies  
110 have sought to examine both biochemical and immunohistochemical quantification of A $\beta$  and tau  
111 pathology within the same cases, thus, allowing for a direct comparison between the correlative  
112 strength of total A $\beta$ , plaque A $\beta$  and intracellular A $\beta$  with tau pathology. This current study aimed to  
113 quantify such parameters across cases to establish potential correlative relationships between  
114 pathological species in order to further understand the influence that A $\beta$ , in various forms, may have  
115 upon the regional generation of tau pathology, both in neuropathologically confirmed cases of AD as  
116 well as non-AD control cases.

117

## 118 **Methods**

### 119 **Human post-mortem brain tissue**

120 A study cohort of post-mortem human brains from clinico-pathologically classified AD (n=21) and non-  
121 neurodegenerative control cases (Con, n=39) was obtained from the Newcastle Brain Tissue Resource  
122 (NBTR). AD Subjects had been clinically assessed during life prior to brain tissue donation and  
123 diagnosed with dementia due AD. Control cases similarly had been assessed during life and at the time

124 of death did not have dementia. The final clinico-pathological diagnoses were established by  
125 combining clinical neuropathological data reviewed at regular meetings involving JA and AT.  
126 Neuropathological diagnoses were based on assessment of brain tissue according to the National  
127 Institute of Ageing – Alzheimer’s Association (NIA-AA) criteria[38], including Braak NFT staging[39],  
128 Thal phases [6], and Consortium to Establish a Registry for Alzheimer’s Disease (CERAD) scoring[40],  
129 as well as Braak LB stages[41], and Newcastle / McKeith Criteria [42, 43] (Table 1 and S1 for full  
130 details).

131 For histology and tissue micro-array (TMA; see below), tissue sections were prepared from the right  
132 hemisphere of the brain and fixed for 4-6 weeks in 4% paraformaldehyde. Corresponding frozen  
133 frontal grey (GM) and white matter (WM) tissue (Brodmann’s area (BA) 9) was obtained from the left  
134 hemisphere, dissected in a coronal plane and snap frozen between copper plates at -120°C prior to  
135 being stored at -80°C. Due to limitations in tissue availability, it was not possible to obtain both fixed  
136 and frozen tissue for all cases (see Table 1 and S1 for full details). Comparative analysis of age and  
137 post-mortem interval (PMI) between disease groups determined no significant difference in either  
138 measure ( $p>0.05$ ).

139

#### 140 **Tissue lysis**

141 ~250mg of frozen frontal tissue was electronically homogenised 1:10 (W/V) in 0.2M tetraethyl  
142 ammonium bicarbonate (TEAB, pH 7.2, Sigma) with 1% SDS, containing protease (1 per 10ml,  
143 Complete , Roche) and phosphatase inhibitors (1 per 10mls, PhosSTOP, sigma) using an Ultra-turrax  
144 T10 homogeniser (5 mm diameter probe; 30,000rpm) for 15 sec. Lysate were aliquoted and stored at  
145 -80°C, prior to use.

146

#### 147 **Immunoblot quantification of AD markers:**

148 Dot blots were conducted for total A $\beta$  and AT-8 phospho-tau in both grey and white matter samples.  
149 The protein concentration of GM and WM crude lysate were adjusted to 0.5 $\mu$ g/ $\mu$ l as per Bradford assay  
150 and dotted directly to a nitrocellulose membrane at 10 $\mu$ l (5 $\mu$ g/dot) and left to dry for 20 minutes  
151 before further processing. The membranes, briefly washed in Tris-buffered saline (TBS; in mM; 50  
152 Trizma base, 150 NaCl, pH= 7.6) prior to being blocked in 5% milk powder containing Tris-Buffered  
153 Saline with 0.1% Tween 20 (TBST) at room temperature for 1 hour. After blocking, blots were rinsed  
154 in TBS washing buffer 3 times for 5 minutes each. Membranes were subsequently placed in primary  
155 antibody solution (TBST, 5% bovine serum albumin and 0.05% sodium-Azide) containing either MOAB-

156 2 (1:1000, Cat# M-1586-100, Biosensis) for the detection of A $\beta$  or AT-8 (1:1000, Cat# AB\_223647,  
157 Thermofisher) for phospho-tau and incubated overnight at 4°C. The membranes were then washed  
158 in TBST before being incubated for 1 hour at room temperature in horse radish peroxidase conjugated  
159 goat anti-mouse secondary IgG antibody (TBST+5% milk powder+1:5000 dilution) prior to repeated  
160 washing before being development. Immunoreactivity was visualized via enhanced  
161 chemiluminescence (1.25 mM Luminol, 25 $\mu$ l of 3% H<sub>2</sub>O<sub>2</sub> and 50 $\mu$ l coumaric acid was incubated for 1  
162 minute). The signal was captured by using digital western blot camera, with high sensitivity and auto  
163 exposure being selected. The images were saved as 8-bit for illustration and 16-bit for quantification.  
164 Total protein loading was determined via Ponceau S general protein stain (0.1% Ponceau S (w/v) and  
165 5.0% acetic acid (w/v) in ddH<sub>2</sub>O water) and resulting loading staining captured.

#### 166 **Immuno-blot quantification**

167 Immunoreactivity of enhanced chemiluminescent (ECL) luminol blots and Ponceau S-stained blots was  
168 quantified from 16-bit digitized images based on area under the curve measurements as computed by  
169 ImageJ (Ver 1.53e, NIH, USA). Normalization of immunoblot intensity values were then performed  
170 using total protein adjusted values. The 52 samples of human frontal cortex GM and WM were  
171 processed in 4 separate batches and each batch normalized to the mean value of control cases (each  
172 blot containing >3 Br 0-IV control cases) prior to pooling values between blots.

173

#### 174 **Immunohistochemical quantification of A $\beta$ plaques and phospho-tau (AT-8)**

175 Regional quantification of the A $\beta$  plaque and AT-8 phospho-tau load within the frontal cortex (BA9)  
176 via TMA slides, as described previously[44]. Sections (6  $\mu$ m, thick) were cut from paraffin embedded  
177 TMA blocks tissue blocks comprising of cylindrical tissue cores taken from multiple brain region  
178 specific blocks and mounted on glass slides. Slides containing a 3 mm diameter samples of BA9 frontal  
179 cortex were baked at 60°C for 1hr prior to being dewaxed in xylene, rehydrated in descending  
180 concentration of ethanol (5 mins immersion) and washed in TBS. Slides intended for phospho-tau  
181 staining were treated with microwave assisted antigen retrieval (800 W, 10 mins) in citrate buffer (10  
182 mM Citric acid, 0.05 % Tween 20, pH 6) and those intended for A $\beta$  plaque staining were submerged in  
183 90% Formic acid for 1hr at RT, before endogenous peroxidases were quenched in H<sub>2</sub>O<sub>2</sub> (3%, 20 mins  
184 submersion). Following consecutive washes in TBS and TBST, slides were incubated with either mouse  
185 4G8 (1:16000, Cat# SIG-39200, Covance) or anti-AT-8 (1:4000) in TBS for 1 hr and immunoreactivity  
186 visualised via the MENAPATH HRP polymer detection kit (Menarini diagnostics, Wokingham, UK) and  
187 3,3'- Diaminobenzidine (DAB) chromogen with appropriate TBS and TBST washes performed between

188 steps. Slides were co-stained with haematoxylin prior to being dehydrated in ethanol, cleared in  
189 xylene and mounted in dibutylphthalate polystyrene xylene (DPX).

190 Stained BA9 frontal cortex samples were imaged at x100 magnification with a semi-automated  
191 microscope (Nikon Eclipse 90i microscope, DsFi1 camera and NIS elements software V 3.0, Nikon). For  
192 each case, multiple images were captured to form a 3x3 image grid with 15% overlap in adjacent  
193 images, such that an area of 1.7mm was sampled from each case.

194 Following visual quality control inspection and the application of regions of interest (ROI) to exclude  
195 areas of tissue folds and tears, a consistent restriction threshold for 4G8 (R50-180, G20-168, and B8-  
196 139) and AT-8 (R25-170, G27-156, B11-126) was applied producing a binary signal image from which  
197 the percentage area of immunoreactivity could be acquired. For the quantification of A $\beta$  plaques, 4G8  
198 images were further processed by means of size exclusion, restricting object detection to >100 $\mu$ m<sup>2</sup>,  
199 thus avoiding inclusion of intracellular APP and A $\beta$ .

200

#### 201 **Immuno-fluorescent histochemical analysis of intracellular A $\beta$ and phospho-Tau (AT-8)**

202 Paraffin embedded tissue blocks of the frontal cortex BA9 were used to prepare sections (6  $\mu$ m thick)  
203 for the purpose of multiplex intracellular A $\beta$  and phospho-tau fluorescent staining. Slide mounted  
204 frontal cortex sections were baked at 60°C for 1hr, dewaxed and rehydrated and subjected to antigen  
205 retrieval in citrate buffer and formic acid treatment (as above). Slides were then blocked in TBST  
206 containing 10% normal goat serum for 1hr at RT and incubated in mouse IgG2b anti-MOAB-2 and  
207 mouse IgG1 anti-AT-8 (1:500, for both) overnight at 4°C, prior to incubation in secondary antibodies  
208 (goat-anti mouse IgG1 – Alexa 488 and goat-anti mouse IgG2b-Alexa 594, 1:1000 for both, Invitrogen).  
209 Endogenous tissue fluorescent was quenched via post-staining treatment with Sudan Black (0.01%,  
210 70% ethanol, 5mins submersion) before slides were coverslipped with DAPI-containing Prolong  
211 Diamond Mounting media (Fisher Scientific). In a subset of slides, the limited co-localization of MOAB-  
212 2 labelled A $\beta$  and APP was established, staining sections with mouse- IgG2b anti-MOAB-2 and Rabbit-  
213 anti-APP (1:500, Cat# ab15272, abcam) and appropriate secondary antibodies. Fluorescence antibody  
214 labelled sections were imaged via a wide-field fluorescence microscope system (Nikon Eclipse 90i  
215 microscope, DsQi1Mc camera and NIS elements software V 3.0, Nikon).

216 One section per case was examined at 400x magnification with 3 images per grey matter and white  
217 matter region selected at random. As these images were used for quantification of intracellular A $\beta$ ,  
218 excluding A $\beta$ -plaques, any region selected which contained multiple plaques was excluded and  
219 another region selected. ROI were manually applied to each image and folds, tears and plaques were



220 excluded, before images were converted to grey scale and a consistent threshold applied to generate  
221 a binary image from which percentage area of immunoreactivity was determined. The mean  
222 percentage area of immunoreactivity was calculated per grey and white matter area per case.

223

## 224 **Data analysis**

225 Data were subjected to Shapiro-Wilk normality test for normal distribution, prior to statistical  
226 comparison between control and AD cases using a non-parametric Mann-Whitney U test (GraphPad  
227 Prism Ver. 5). In SPSS, two-tailed Spearman's correlation was used for correlation analysis. Given the  
228 association of increasing Braak stage with age, all correlations with Braak staging were performed with  
229 partial correlations controlling from age. A series of one- tailed t-test were performed to identify the  
230 initial stage at which measures were significantly elevated from Braak 0 pathological controls. For all  
231 analysis,  $p < 0.05$  was considered as statistically significant, with increasing statistical reliability for  
232  $p < 0.01$ ,  $p < 0.001$  and  $p < 0.0001$ .

233

## 234 **Results**

### 235 **Biochemical analysis of A $\beta$ and phospho-tau pathology.**

236 In order to limit the potential confounding influence of age-related A $\beta$  independent tau pathology as  
237 seen in PART[12], Brodmann's area 9 of the superior frontal cortex, a region which does not develop  
238 NFTs until late stage of AD related disease progression (Braak NFT V-VI) was selected for investigation.  
239 Using a native state dot-blot quantification, crude tissue lysates of grey matter of this region as well  
240 as the associated white matter of AD (n=17) and non-AD controls (n=35), were probed for A $\beta$  via the  
241 non-APP cross-reactive MOAB-2 antibody and for tau pathology using the phospho-tau specific  
242 antibody AT-8.

243 When considered purely based on the neuropathological diagnosis of either non-AD and AD, levels of  
244 AT-8 phospho-tau were elevated in AD cases, both in GM ( $13.24 \pm 3.3$ -fold cf. non-AD,  $p < 0.001$ , fig1 a.i  
245 + b.i) and WM ( $9 \pm 2.6$  fold cf. non-AD,  $p < 0.001$ , fig1 a.i + b.i). Despite a numerically higher mean within  
246 the GM compared to the WM, there was no statistically significant difference between the magnitude  
247 of increase between GM and WM in AD cases ( $p > 0.05$ ). Similarly, when A $\beta$  levels were examined based  
248 on the neuropathological cohort stratification of Non-AD and AD, elevations were apparent within the  
249 GM ( $3.35 \pm 0.59$  fold c.f non-AD,  $p < 0.01$ , fig1 a.ii + c.ii) and WM ( $2.56 \pm 0.56$  fold c.f non-AD,  $p < 0.05$ , fig1  
250 a.ii + b.ii) of AD cases. Again, no difference between the magnitude of increase within AD cases relative  
251 to control cases was observed between GM and WM ( $p > 0.05$ ).

252 Such an outcome from the analysis of phospho-tau and A $\beta$  between AD and non-AD cases is not  
253 surprising but serves to validate the use of dot-blot to measure biochemical changes in phospho-tau  
254 and A $\beta$ .

255 To further place the observed changes of tau and A $\beta$  within the context of disease progression, the  
256 cohort was subdivided into their respective Braak stages (0-VI) and the association of crude lysate  
257 measures of AT-8 phospho-tau and A $\beta$  with disease progression was determined (Fig 1 c.i + ii).  
258 Phospho-tau AT-8 immunoreactivity correlated with increasing Braak stages when considered across  
259 the entire cohort within the GM ( $r=0.7$ ,  $p<0.001$ ) as well as in the WM ( $r=0.67$ ,  $p<0.001$ ). Additionally,  
260 a modest but significant correlation between Braak NFT stage and age was reported ( $r=0.34$ ,  $p<0.05$ )  
261 although age did not correlate with biochemical measures of AT-8 ( $p>0.05$ , data not shown).  
262 Correlations between AT-8 immunoreactivity and Braak NFT remained when adjusting for age ( $r=0.62$   
263 and  $r=0.57$  for GM and WM respectively,  $p<0.001$  for both, fig 1 c). Interestingly when probed for the  
264 stage at which phospho-tau levels were significantly elevated from that of “pathologically-free” Braak  
265 stage 0 cases, Braak stage IV was indicated ( $p<0.05$ , for both GM and WM). Braak stage IV being the  
266 stage prior to gross affection of the frontal cortex with NFTs. Furthermore, when split according to  
267 neuropathological diagnosis, and controlled for age, a significant correlation was observed in the non-  
268 AD control group in GM (Fig 1 c.i,  $r=0.47$ ,  $p<0.01$ ) and WM (Fig 1c.i,  $r=0.43$ ,  $p<0.05$ ), but not in AD  
269 cases (Fig 1 c.i,  $p>0.05$ ). Together the data suggest that in non-AD control cases, AT-8 phospho-tau  
270 increases within the frontal cortex in line with the intra-regional spatial AT-8 positive NFT progression,  
271 somewhat independent of age. Thus, initial levels of frontal cortex AT-8 positive phospho-tau may be  
272 regionally generated.

273 Following a similar line of investigation for the accumulation of A $\beta$  in relation to disease progression,  
274 A $\beta$  levels were correlated with individual Braak NFT stages. Across the entire cohort, robust  
275 correlations were reported for both the GM ( $r=0.67$ ,  $p<0.001$ , fig 1 d) and WM ( $r=0.6$ ,  $p<0.001$ , fig 1  
276 d). Again, correlations remained when controlling for age ( $r=0.54$  and  $r=0.53$  for GM and WM  
277 respectively,  $p<0.001$  for both). In line with observations of AT-8 phospho-tau, individual comparisons  
278 with Braak 0 cases reported an initial significant elevation from the “pathologically-free” baseline at  
279 Braak 4, in GM and WM samples ( $p<0.05$ ). Consistent with similar measures of AT-8 phospho-tau,  
280 when divided into non-AD and AD categories, increasing total A $\beta$  correlated with progressive Braak  
281 stages in the non-AD group in both the GM and WM ( $r=0.36$ ,  $p<0.05$  and  $r=0.46$ ,  $p<0.01$  in GM and  
282 WM respectively, fig 1 d) and not in the AD group ( $p>0.05$ ). Similar to correlation with Braak staging,  
283 all other neuropathological classifications also reported robust correlations when considered as a  
284 single cohort (See S.table 2). When considering Non-AD controls only, significant correlation with AT8  
285 phospho-tau was only apparent with CERAD scores for GM and WM ( $r=0.4$ ,  $p<0.05$  and  $r=0.47$ ,

286 p<0.001, respectively) whilst GM and WM scores for A $\beta$  correlated with Thal, CERAD and NIA-AA  
287 (r=0.38-0.52, p<0.05, see S.table 2 for full details). In terms of AD cases, correlations were apparent  
288 for all biochemical measures with all neuropathological scheme (see S.table 2).

289 Collectively, the data suggest a robust relationship of AT-8 and A $\beta$  with disease progression within the  
290 GM and WM of the frontal cortex, occurring not only in confirmed cases of AD but also non-AD  
291 controls. In the frontal cortex, intra-regional pathology progresses in accordance with global AD-  
292 related brain tau pathology as quantified by Braak NFT stages and this was most evident in non-AD  
293 controls.

294 Independent of global brain AD related pathological changes, a critical element to regional pathology  
295 is to determine whether biochemical measures of tau pathology and A $\beta$  correlate on a case-by-case  
296 basis, as the disconnect of histochemical tau and A $\beta$  pathological hallmarks has long been a major  
297 caveat to the amyloid cascade hypothesis. Indeed, a robust correlation between biochemical  
298 measures of AT-8 phospho-tau and total A $\beta$  measures was observed when considered as a single  
299 cohort (Non-AD + AD cases) in the GM (r=0.75, p<0.001, fig 1 d.i) and in the WM (r=0.67, p<0.001, fig1  
300 e.i). Remarkably, when examined separately within Non-AD controls and AD cases, correlations  
301 between AT-8 phospho-tau and A $\beta$  were apparent in both control cases (GM; r=0.52, p<0.001 and  
302 WM; r=0.67, p<0.001, fig 1 d ii + e ii) as well as AD cases (r=0.5, p<0.05 and r=0.73, p<0.01 in GM and  
303 WM, fig 1 d iii + e iii).

304

### 305 **Histochemical quantifications of AT-8 phospho-tau and A $\beta$ plaques.**

306 In order to establish if the biochemical derived relationship of increased in A $\beta$  immunoreactivity  
307 conferring increased in AT-8 immunoreactivity was primarily driven by an association of A $\beta$  plaques  
308 with AT-8 phospho-tau, semi-quantitative immunohistochemistry analysis was performed (Fig 2 a, and  
309 see S.table 1 for details). Based on % area coverage, AT-8 immunoreactivity, a composite of NFTs and  
310 NTs reported a marked ~ 100 fold increase in % coverage in the frontal grey matter of AD cases  
311 compared to controls (7.6 $\pm$ 2.5% vs. 0.07 $\pm$ 0.02%, in AD and non-AD cases respectively, p<0.001, fig 2  
312 b.i). Equally, quantification of the % area coverage of A $\beta$  plaques between AD cases and non-AD  
313 controls, also, unsurprisingly reported a significant increase with the AD cases (14.26 $\pm$ 1.7% cf.  
314 3.55 $\pm$ 1%, p<0.001, fig 2 b.ii).

315 When measures were considered in relation to progressive Braak NFT staging, AT-8 phospho-tau  
316 (r=0.55, p<0.001, fig 2 c.i) and A $\beta$  plaques (r=0.67, p<0.001, fig 2 c.ii) strongly correlated with Braak  
317 stage, following a correction for age. Again, a significant elevation in AT-8 phospho-tau and A $\beta$  plaque

318 coverage from “pathologically-free” Braak stage 0 cases was reported at Braak Stage IV ( $p < 0.05$ ), in  
319 line with observations from biochemical measurements. When controlling for age, no significant  
320 correlations were observed for AT-8 phospho-tau or A $\beta$  plaques for either non-AD or AD groups  
321 ( $p > 0.05$ ). Further analysis with additional neuropathological classification reported strong correlations  
322 with Thal and CERAD and NIA-AA when considered as a single cohort and in control only (S.table 3).  
323 Collectively, the data largely suggests that correlative relationships reported within the overall cohort  
324 likely stems from group effects driven by the general increase of pathological hallmarks between non-  
325 AD and AD groups and not as incremental regional increase in line with progressive Braak stage. Such  
326 observations contrast with the findings of the biochemical investigation.

327 Equally correlations between IHC quantified A $\beta$  and AT-8 phospho-tau also reported a correlation only  
328 when the data were analysed as a single cohort combining non-AD controls and AD cases ( $r = 0.65$ ,  
329  $p < 0.001$ , fig 2 d) and not when examined as a separate data set of non-AD controls or AD cases  
330 ( $p > 0.05$ , for both, fig 2 dii+iii). Nevertheless, biochemical measures correlated with respective  
331 histochemical measures for AT-8 and A $\beta$  (see Stable 4). Thus, despite the contradiction between  
332 biochemically measured association of AT-8 phospho-tau and total A $\beta$  and histologically measured AT-  
333 8 phospho-tau and A $\beta$  plaque load, the measures by differing methodological means are somewhat  
334 inter-related.

335

### 336 **Quantification of intracellular A $\beta$**

337 The absence of a correlation between IHC measures AT-8 and plaques (fig 2), despite a robust  
338 correlation with of biochemical AT-8 and total A $\beta$  measures from crude tissue lysates (fig 1), suggests  
339 the possible inclusion of additional A $\beta$  sources within the biochemical quantification. Accordingly, the  
340 application of MOAB-2 A $\beta$  antibody to fixed post-mortem human brain tissue sections, labelled both  
341 extracellular plaques and intracellular pools of A $\beta$  (fig 3). Comparisons of APP and MOAB-2 A $\beta$   
342 labelling, demonstrated a clear distinction in subcellular and plaque labelling in both GM (fig 3 a) and  
343 WM (fig 3 b). Whilst there is a degree of overlap as would be expected given the spatial limitation and  
344 the production of A $\beta$  from APP, co-localisation is absence in the majority of puncta (fig 3; white  
345 arrows), confirming the specificity of MOAB-2 for the labelling of A $\beta$ , as previously reported[45, 46].  
346 Across a subset of the cohort, both in the GM and WM, a progressive increase in intracellular A $\beta$   
347 staining in line with increase AT-8 immunoreactivity was observed (fig 4.a). When intracellular A $\beta$  was  
348 quantified according to % area coverage, a significant increase in the levels was observed in AD cases  
349 compared to controls (fig 4b.i,  $p < 0.001$  in GM and  $p < 0.05$  in WM). Similarly, AT-8, as measured by  
350 immunofluorescence was again elevated in AD cases (fig 4 b ii,  $p < 0.001$  in GM and WM). Both AT-8

351 (r=0.62, p<0.01 in GM and r=0.5, p<0.05 in WM) as well as intracellular A $\beta$  (r=0.61, p<0.01 in GM)  
352 correlated with Braak stage when controlling for age. Equally, strong correlations were observed with  
353 Thal, CERAD and NIA-AA also (see S.table 5). No correlations with any neuropathological classifications  
354 were reported when the cohort was spilt according to Non-AD and AD groups. Nevertheless,  
355 correlative measures between intracellular A $\beta$  and AT-8 phospho-tau reported a significant  
356 relationship across all cases (in GM, r=0.76 and in WM, r=0.71, p<0.01 for both, fig 4 c i + d i,) and in  
357 control cases only (in GM, r=0.82 and in WM, r=0.76, p<0.01 for both, fig 4 c ii + d ii). Interestingly  
358 when considering only the AD cases, a significant inverse correlation of intracellular A $\beta$  with AT-8  
359 phospho-tau in the GM, was apparent (r=-0.74, p<0.05, fig 4 c iii), although no correlation was  
360 reported in the WM (fig 4 d iii). As with IHC quantifications of plaques and AT-8 as per TMA slides,  
361 measures of intracellular A $\beta$  and AT-8 here, also correlated with biochemical measures when  
362 considered as a single group, although no significant correlations were observed when split into  
363 Control and AD categories (S. table4).

364 Collectively quantification of the intracellular A $\beta$  and its correlation with AT-8 phospho-tau appears  
365 to support the biochemical findings of a close relationship between AT-8 and A $\beta$ , particularly in non-  
366 AD control cases. However is should be noted that spatial colocalization of AT-8 and intracellular A $\beta$   
367 was not common and appeared to be the exception rather than the rule (fig 5), instead here we find  
368 a correlation of regional AT-8 burden with regional intracellular A $\beta$ .

369

## 370 **Discussion**

371 Collectively this study reports an apparent correlation between biochemical A $\beta$  and AT-8 phospho-tau  
372 measures. Such a relationship was not reproduced when comparing IHC based quantification of A $\beta$   
373 plaques and AT-8 phospho-tau but was observed when considering IHC measures of phospho-tau and  
374 intracellular A $\beta$ . These correlative relationships are perhaps surprisingly strongest within the non-AD  
375 control group and are evident in both grey and white matter. Together the data suggests a close  
376 relationship between non-plaque A $\beta$  and tau, which is at least partially due to the accumulation of  
377 intracellular A $\beta$  and its potential influence on tau phosphorylation.

378

379

380

## 381 **Regional correlation of tau and A $\beta$**

382 A long-standing critique of the amyloid cascade hypothesis has been the disconnect between NFT and  
383 A $\beta$ -plaque burden within a given brain region of either non-AD controls or indeed AD cases [47, 48].  
384 However many biochemical approaches have previously found correlations between A $\beta$ , either total  
385 A $\beta$  or specifically A $\beta$ <sub>1-42</sub>, with a range of phosphorylated and oligomeric tau markers within the GM  
386 of a given cortical region[14-17]. Furthermore, disease dependent changes in white matter A $\beta$  levels  
387 have also been previously observed using A $\beta$ <sub>40</sub> and A $\beta$ <sub>42</sub> ELISAs[49] and like-wise hyperphosphorylated  
388 tau has also been observed biochemically within the white matter of AD cases[13, 50]. Here we  
389 observed that levels of AT-8 reactive phospho-tau and A $\beta$  increased in non-AD controls in line with  
390 Braak stage progression, in both the frontal grey and white matter and exhibited a positive correlation  
391 between A $\beta$  levels and AT-8 when measured biochemically. Whilst our observations cannot  
392 determine causality, our findings are consistent with many *in-vitro* experiments in which the  
393 application of A $\beta$  to various cellular preparations results in downstream tau phosphorylation[28, 51,  
394 52]. Moreover, support for the interaction of A $\beta$  with tau pathology, can be gained from studies  
395 reporting that interventions targeting A $\beta$  levels consequently reduce tau pathology both *in-vitro* and  
396 *in-vivo* models[53, 54] as well as in biofluids obtained from human clinical trials[3, 4, 55].

397 When considering the association of A $\beta$  and tau phosphorylation within non-AD controls, our findings  
398 are similar to the observation of a previously seen correlation between A $\beta$ <sub>1-40</sub> level and p-181 tau in  
399 the CSF of control cases[56]. However here we can extend this finding to show that within the frontal  
400 cortex there is a regional dependence between A $\beta$  levels and tau pathology. As work by others have  
401 reported no or minimal seed competent tau within the frontal cortex in non-AD controls [50], the  
402 source of pathology within the frontal cortex is likely to mainly be intraregional, with minimal  
403 influence of extra-regional spread. Such intraregional dependence would be consistent with the  
404 strong correlation between A $\beta$  and AT-8 signals within the non-AD controls, which is somewhat  
405 weakened in AD cases, when seed competent tau species have presumably invaded the frontal  
406 cortex[13], the self-propagation of tau pathology thus diminishing the relative contribution of A $\beta$  to  
407 the production of phospho-tau species. Interestingly, a linear relationship between regional soluble  
408 tau phospho-species and A $\beta$ <sub>1-42</sub> has previously been reported alongside a bimodal relationship within  
409 the insoluble fraction, implying a weakening of the relationship between A $\beta$ <sub>1-42</sub> and tau  
410 phosphorylation once aggregated [17]. Thus, given that this present study did not seek to distinguish  
411 between soluble and insoluble pathology, the increased representation of insoluble tau pathology  
412 within lysates from AD cases, likely further explains the weakening of the linear relationship between  
413 A $\beta$  and tau phosphorylation in AD cases.

414 Accordingly, no linear correlation was observed between plaque load and AT-8 load when measured  
415 histologically. Such differences may relate to the presumed loss of extracellular soluble A $\beta$  and

416 exclusion of intracellular A $\beta$  pools, as is common practice when assessing A $\beta$  burden as part of a  
417 neuropathological assessment[44].

418

#### 419 **Intracellular A $\beta$**

420 Historically, intracellular A $\beta$  has been problematic in its quantification, largely due to the cross-  
421 reactivity of A $\beta$  antibodies with APP and other intermediate APP metabolites. However, several  
422 commercial A $\beta$  antibodies are available, including MOAB-2 which shows no cross-reactivity with APP  
423 under many conditions [45, 46].

424 Although often overlooked, the production of A $\beta$  occurs intracellularly following endosomal APP  
425 cleavage via  $\beta$ -secretase [57] and sequential  $\gamma$ -secretase processing within either Golgi [58] or  
426 lysosomal [59] compartments. Whilst the majority of A $\beta$  is trafficked to the extracellular space, age-  
427 related changes in the relative production of A $\beta$  peptide length [60] and disease alterations to  
428 trafficking mechanisms, such as Rab GTPases [61, 62], may act synergically to enhance the retention  
429 of intracellularly produced A $\beta$  and or indeed its reuptake, leading to its intracellular accumulation [63].  
430 Accordingly, post-mortem examination of the entorhinal cortex and hippocampus of non-diseased  
431 non-AD cases, suggests an increase in intracellular A $\beta$  in line with increasing age [64, 65] and  
432 furthermore AD animal models also show an age-related accumulation of intracellular A $\beta$  [46, 66].

433

#### 434 **Intracellular A $\beta$ and tau**

435 Here, when selectively measuring intracellular A $\beta$ , a positive correlation between A $\beta$  and AT-8 in the  
436 frontal cortex of non-AD controls was observed. This is consistent with biochemical measures of  
437 frontal cortex lysates in the same cases as present here or indeed previously reported biochemical  
438 measures in the lateral temporal cortex of a different study cohort[15]. However, in work by others,  
439 no such relationship has been observed in the entorhinal cortex [64][67]. Such a contrast in  
440 relationships may relate to the regions selected for investigation. The entorhinal cortex is one of the  
441 earliest affected cortical regions with tau pathology in AD, and thus presumably represents a cortical  
442 area of increased vulnerability to tau pathology. Such vulnerability may mean that tau pathology may  
443 be generated in an A $\beta$  independent manner within the region as is the case of primary age-related  
444 tauopathy [12]. Nevertheless, within the prefrontal cortex, a region which does not demonstrate  
445 robust age related NFT tau pathology and is not burdened with NFTs until late into the Braak NFT  
446 staging criteria (Braak V-VI), such modest pre-tangle tau-pathology generated in this region may be  
447 largely dependent on A $\beta$  mediated mechanism. Such a mechanism may become modified under

448 pathological conditions, either upon reaching a critical threshold of intracellular A $\beta$  accumulation  
449 and/or via seed component invasion.

450 Interestingly within the grey matter, although a positive relationship between intracellular A $\beta$  and  
451 phospho-tau was observed in non-AD control cases, an inverse relationship was observed in AD cases.  
452 Whilst intracellular A $\beta$  levels remained elevated compared to controls, there has been reports of a  
453 reduction of intracellular A $\beta$  levels in line with the deposition of A $\beta$  plaques in mice models [68] as  
454 well as in serial observations in Down's syndrome brains [69] and cases of late stage NFT mediated  
455 neurodegeneration [67]. Such contradictions may be due to differences in the specific regions of  
456 investigations. However, it is equally plausible that elevation of intracellular A $\beta$  precedes and indeed  
457 acts as a source for extracellular plaque deposition, with the excessive deposition of plaques at later  
458 stages subsequently reducing intracellular A $\beta$  levels as observed in animal model [68]. In turn tau  
459 pathology may continue to grow due to the influence of seed component species.

460 In any case, excessive intracellular A $\beta$  accumulation, is unlikely to be benign. The familial Osaka E639 $\Delta$   
461 APP mutant which produces non-fibril E22 $\Delta$  A $\beta$  gives rise to an accumulation of intracellular A $\beta$   
462 oligomers in the absence of plaques. In AD patients or mouse models carrying the Osaka mutation,  
463 pronounced cognitive impairments, cellular stress, synaptic spine loss and critically pathological tau  
464 phosphorylation and conformational changes are observed [22, 45]. Whilst several of the downstream  
465 cellular dysfunction may be independent of tau [70], these studies nevertheless highlight the induction  
466 of tau pathology via A $\beta$  independent of plaque formation, in support of the observed correlation of  
467 intracellular A $\beta$  and phospho-tau observed here.

468 Given emerging evidence from clinical A $\beta$  antibody trials[71], which supporting the targeting of soluble  
469 fibrillar A $\beta$  species to consequently reduce tau pathology, further understanding the degree of  
470 interaction between A $\beta$  and tau will provide greater insight into the mechanisms of AD related  
471 pathogenesis. Equally, in light of the facilitation of fibril seeding by the existence of pre-existing tau  
472 phosphorylation/pathology in mice [72-74], the targeting of pre-tangle soluble tau elevations in late  
473 stage affected brain regions, may protect against tau seed infiltration as part of AD disease  
474 progression, and may provide an effective stalling of the condition.

475

476

477

478



479 **Conclusions**

480 Collectively this study demonstrates the robust correlation of AT-8 reactive tau and A $\beta$  in the frontal  
481 cortex of both non-AD controls and AD cases when measured biochemically. Given that such linear  
482 increases in A $\beta$  plaques and AT-8 pathology is not observed when quantified via IHC, the study  
483 demonstrates the potential influence of non-plaque A $\beta$  in the intra-regional generation of tau  
484 pathology. Specifically, the occurrence and accumulation of intracellular A $\beta$ , in line with AD  
485 pathological progression, at least in part correlated with AT-8 pathology and thus may contribute to  
486 production of tau pathology. This finding is supportive of the amyloid cascade hypothesis, yet in late-  
487 stage AD cases such a relationship may be diminished, with additional factors contributing to tau  
488 pathology, at least within the frontal cortex. Critically, the observation of a localised relationship  
489 between A $\beta$  and phospho-tau in cases with low Braak NFTs stages implies that there is a degree of  
490 regionally generated AD related pathology, which may be tolerated within a physiological range.  
491 Following the age-related accumulation of pathology, this regionally produced burden may prime the  
492 region for the invasion of seed competent forms of tau originating from connected regions, raising the  
493 burden beyond a critical threshold, and thus removing the necessity of A $\beta$  for the propagation of tau  
494 pathology.

495

496 **Acknowledgements**

497 issue for this study was provided by the Newcastle Brain Tissue Resource which is funded in part by a  
498 grant from the UK Medical Research Council (G0400074), by NIHR Newcastle Biomedical Research  
499 Centre awarded to the Newcastle upon Tyne NHS Foundation Trust and Newcastle University, and as  
500 part of the Brains for Dementia Research Programme jointly funded by Alzheimer's Research UK and  
501 Alzheimer's Society

502

503

504

505

506

507

508

509 Legends

510 Table legends

511 **Table 1. Post-mortem human tissue cases and use.** Human cases use for immuno-blots and  
512 immunohistochemistry for plaques and AT-8 as well as intracellular A $\beta$  and AT-8 are listed. Case are  
513 separated by disease classification according to non-diseased controls (Con) and Alzheimer's disease  
514 (AD). Case numbers (n), sex, age, post-mortem interval (PMI), neurofibrillary tangle (NFT) Braak stage,  
515 Thal phase, Consortium to Establish a Registry for Alzheimer's Disease (CERAD), the National Institute  
516 of Ageing – Alzheimer's Association (NIA-AA) criteria, Lewy body (LB) Braak stage and McKeith criteria  
517 are provided. For age and PMI both range and mean  $\pm$ SEM are provided. For numerical scores of  
518 pathology, range and percentage composition are given. For CERAD scores, negative (neg), A and B  
519 reported. For NIA-AA, not, low and intermediate (inter) risk for Alzheimer's disease. For McKeith  
520 criteria, only percentage composition is given, where cases free of LBs (No LB), brainstem, Limbic and  
521 neocortical (Neo) predominate are indicated.

522

523 Figure legends

524 **Figure 1. Biochemical quantification of AT-8 phospho-tau and A $\beta$  in the frontal cortex of non-AD and**  
525 **AD cases.** A). Example dot blots of AT-8 (i) and MOAB-2 (A $\beta$ ; ii) immunoreactivity and associated  
526 ponceau total protein stain, produced from crude tissue lysates of frontal grey (GM) and white matter  
527 (WM) in control (Con; black lettering) and Alzheimer's disease (AD; red lettering) cases. Braak NFT  
528 stage of each sample is shown. B). Comparison of mean AT-8 (i) and A $\beta$  (ii) immunoreactivity between  
529 control (Con) and Alzheimer's disease (AD) cases in the GM and WM C). Association of AT-8 (i) and A $\beta$   
530 (ii) immunoreactivity with Braak NFT stages across the cohort in GM and WM. Correlative analysis  
531 (Spearman's  $r$ ) is shown for when analysis as a single group or when separated into Con and AD groups.  
532 Combined (i), Con(ii) and AD (iii), linear correlations between AT-8 and A $\beta$  in the GM (D) and WM(E).  
533 Immunoreactive shown as relative to control (Rel. Control). \*= $p$ <0.05, \*\*= $p$ <0.01, \*\*\*= $p$ <0.001 and  
534 \*\*\*\*= $p$ <0.0001. \$ denotes initial Braak NFT stage at which immunoreactivity is significantly elevated  
535 from Braak 0 controls.

536

537

538

539

540 **Figure 2. Immunohistochemical quantification of AT-8 tau and A $\beta$  plaque burden in the frontal**  
541 **cortex of non-AD and AD cases.** A). Example micrographs of DAB based AT-8 and 4G8 (A $\beta$ )  
542 immunoreactivity, area of quantification following threshold application shown in red. Note the size  
543 exclusion in this parameter of intracellular 4G8 labelling to negate potential APP cross-reactivity. B).  
544 Quantification of % area coverage of AT-8 (i) and plaque (ii) immunoreactivity in control (Con) and  
545 Alzheimer's disease (AD) cases. C). Association of % area coverage of AT-8 (i) and plaques (ii) with  
546 Braak NFT stage with correlative analysis (Spearman's r) shown. Combined(i), Con(ii) and AD(iii), linear  
547 correlations between AT-8 and plaques in the GM (D). N.S = not significant, \*\*\*=p<0.001 and  
548 \*\*\*\*=p<0.0001. \$ denotes initial Braak NFT stage at which immunoreactivity is significantly elevated  
549 from Braak 0 controls. Scale in a = 20  $\mu$ m.

550 **Figure 3. Immunohistochemical distinction between MOAB-2 labelled A $\beta$  and APP immunoreactivity**  
551 **in the frontal cortex of an AD case.** Example micrographs of APP (N-terminal-APP antibody) and A $\beta$   
552 (MOAB-2) from an AD case, in the grey (GM; a) and white matter (WM; b). Note the distinctive labelling  
553 of subcellular pools within insert (white arrows) and differential labelling of plaques (in a) Scale =20  
554  $\mu$ m.

555 **Figure 4. Immunohistochemical quantification of intracellular A $\beta$  and AT-8 tau in the frontal cortex**  
556 **of non-AD and AD cases.** A). Example micrographs of AT-8 phosphorylated tau and MOAB-2 labelled  
557 intracellular A $\beta$  in GM and WM of low (i), intermediate (ii), and high (iii) Braak stage cases. B).  
558 Quantification of intracellular A $\beta$  (i) and AT-8 phospho-tau (ii) expressed as percentage area coverage  
559 in control (Con) and Alzheimer's disease (AD) cases. Combined(i), Con(ii) and AD(iii), spearman's  
560 correlations (r) between AT-8 and plaques in the GM (C) and WM (D). N.S = not significant, \*=p<0.05,  
561 \*\*=p<0.01, \*\*\*=p<0.001 and \*\*\*\*=p<0.0001. Scale =20  $\mu$ m.

562 **Figure 5. Rare instances of intracellular A $\beta$  and tau colocalization.** Example micrographs  
563 demonstrating an overlap of AT-8 and A $\beta$  immunoreactivity within cells from a non-AD control Braak  
564 stage IV. Scale=10  $\mu$ m.

565

566

567

568

569

570

571  
572  
573  
574  
575  
576  
577  
578  
579  
580  
581  
582  
583  
584  
585  
586  
587  
588  
589  
590  
591  
592  
593  
594  
595  
596  
597  
598  
599  
600  
601  
602  
603  
604  
605  
606

Supplemental

**Supplemental table 1 – Individual case list for tissue used.** Each case was assigned an arbitrary case number (Case no) and sex, age (years), post-mortem delay (PMD, hrs), Braak stage, Thal phase, Consortium to Establish a Registry for Alzheimer’s Disease (CERAD), the National Institute of Ageing – Alzheimer’s Association (NIA-AA) criteria, Lewy body (LB) Braak stage and McKeith criteria and tissue use of either biochemical( Biochem) analysis, tissue microarray for plaque and AT-8 pathology (TMA) and immunohistochemistry for intracellular A $\beta$  and AT-8 (IHC) is provided.

**Supplemental table 2. Correlation matrix of biochemical measures of A $\beta$  and AT-8 reactive tau with neuropathological assessment.** Spearman correlations (r) between AT-8 and A $\beta$  and Braak NFT staging, Thal phase, CERAD, NIA-AA, Age and postmortem delay (PMD) are shown for both the grey matter (GM) and white matter (WM) samples. Note for Braak stage correlations reported are controlled for the influence of age. N.S = not significant, \*=p<0.05, and \*\*=p<0.01.

**Supplemental table 3. Correlation matrix of immunohistochemical measures of A $\beta$  plaques and AT-8 reactive tau with neuropathological assessment.** Spearman correlations (r) between AT-8 and A $\beta$  and Braak NFT staging, Thal phase, CERAD, NIA-AA, Age and postmortem delay (PMD) are shown. Note for Braak stage correlations reported are controlled for the influence of age. N.S = not significant, \*=p<0.05, and \*\*=p<0.01.

**Supplemental table 4. Correlation matrix of all measures of A $\beta$  and AT-8 reactive tau across the study** Spearman correlations (r) between AT-8 and A $\beta$  and Braak NFT staging, Thal phase, CERAD, NIA-AA, Age and post-mortem delay (PMD) are shown. Note for Braak stage correlations reported are controlled for the influence of age. N.S = not significant, \*=p<0.05, and \*\*=p<0.01.

**Supplemental table 5. Correlation matrix of immunohistochemical measures of intracellular A $\beta$  and AT-8 reactive tau..** Spearman correlations (r) between AT-8 and A $\beta$  and Braak NFT staging, Thal phase, CERAD, NIA-AA, Age and postmortem delay (PMD) are shown for both the grey matter (GM) and white matter (WM) samples. Note for Braak stage correlations reported are controlled for the influence of age. N.S = not significant, \*=p<0.05, and \*\*=p<0.01.

607

## 608 References

- 609 1. Hardy, J.A. and G.A. Higgins, *Alzheimer's disease: the amyloid cascade hypothesis*. Science, 1992. **256**(5054): p. 184-5.
- 610 2. Hardy, J. and D.J. Selkoe, *The amyloid hypothesis of Alzheimer's disease: progress and problems on the road to therapeutics*. Science, 2002. **297**(5580): p. 353-6.
- 611 3. Cummings, J., et al., *Aducanumab produced a clinically meaningful benefit in association with amyloid lowering*. Alzheimers Res Ther, 2021. **13**(1): p. 98.
- 612 4. McDade, E., et al., *Lecanemab in patients with early Alzheimer's disease: detailed results on biomarker, cognitive, and clinical effects from the randomized and open-label extension of the phase 2 proof-of-concept study*. Alzheimers Res Ther, 2022. **14**(1): p. 191.
- 613 5. van Dyck, C.H., et al., *Lecanemab in Early Alzheimer's Disease*. N Engl J Med, 2023. **388**(1): p. 9-21.
- 614 6. Thal, D.R., et al., *Phases of A beta-deposition in the human brain and its relevance for the development of AD*. Neurology, 2002. **58**(12): p. 1791-800.
- 615 7. Mattsson, N., et al., *Staging  $\beta$ -Amyloid Pathology With Amyloid Positron Emission Tomography*. JAMA Neurol, 2019. **76**(11): p. 1319-1329.
- 616 8. Braak, H. and E. Braak, *Staging of Alzheimer's disease-related neurofibrillary changes*. Neurobiol Aging, 1995. **16**(3): p. 271-8; discussion 278-84.
- 617 9. Braak, H., et al., *Stages of the pathologic process in Alzheimer disease: age categories from 1 to 100 years*. J Neuropathol Exp Neurol, 2011. **70**(11): p. 960-9.
- 618 10. Spires-Jones, T.L., J. Attems, and D.R. Thal, *Interactions of pathological proteins in neurodegenerative diseases*. Acta Neuropathol, 2017. **134**(2): p. 187-205.
- 619 11. Zhang, Y., et al., *Tauopathies: new perspectives and challenges*. Mol Neurodegener, 2022. **17**(1): p. 28.
- 620 12. Crary, J.F., et al., *Primary age-related tauopathy (PART): a common pathology associated with human aging*. Acta Neuropathol, 2014. **128**(6): p. 755-66.
- 621 13. DeVos, S.L., et al., *Synaptic Tau Seeding Precedes Tau Pathology in Human Alzheimer's Disease Brain*. Front Neurosci, 2018. **12**: p. 267.
- 622 14. Näslund, J., et al., *Correlation between elevated levels of amyloid beta-peptide in the brain and cognitive decline*. Jama, 2000. **283**(12): p. 1571-7.
- 623 15. Koss, D.J., et al., *Soluble pre-fibrillar tau and  $\beta$ -amyloid species emerge in early human Alzheimer's disease and track disease progression and cognitive decline*. Acta Neuropathol, 2016. **132**(6): p. 875-895.
- 624 16. Koss, D.J., et al., *Distinctive temporal profiles of detergent-soluble and -insoluble tau and A $\beta$  species in human Alzheimer's disease*. Brain Res, 2018. **1699**: p. 121-134.
- 625 17. Horie, K., et al., *Regional correlation of biochemical measures of amyloid and tau phosphorylation in the brain*. Acta Neuropathol Commun, 2020. **8**(1): p. 149.
- 626 18. Lasagna-Reeves, C.A., et al., *Tau oligomers impair memory and induce synaptic and mitochondrial dysfunction in wild-type mice*. Mol Neurodegener, 2011. **6**: p. 39.
- 627 19. Nicole, O., et al., *Soluble amyloid beta oligomers block the learning-induced increase in hippocampal sharp wave-ripple rate and impair spatial memory formation*. Sci Rep, 2016. **6**: p. 22728.
- 628 20. Bolós, M., et al., *Soluble Tau has devastating effects on the structural plasticity of hippocampal granule neurons*. Transl Psychiatry, 2017. **7**(12): p. 1267.
- 629 21. Koss, D.J., et al., *Polymeric alkylpyridinium salts permit intracellular delivery of human Tau in rat hippocampal neurons: requirement of Tau phosphorylation for functional deficits*. Cell Mol Life Sci, 2015. **72**(23): p. 4613-32.
- 630
- 631
- 632
- 633
- 634
- 635
- 636
- 637
- 638
- 639
- 640
- 641
- 642
- 643
- 644
- 645
- 646
- 647
- 648
- 649
- 650
- 651
- 652
- 653
- 654

- 655 22. Tomiyama, T., et al., *A mouse model of amyloid beta oligomers: their contribution to synaptic*  
656 *alteration, abnormal tau phosphorylation, glial activation, and neuronal loss in vivo.* J  
657 Neurosci, 2010. **30**(14): p. 4845-56.
- 658 23. Busche, M.A., et al., *Critical role of soluble amyloid- $\beta$  for early hippocampal hyperactivity in a*  
659 *mouse model of Alzheimer's disease.* Proc Natl Acad Sci U S A, 2012. **109**(22): p. 8740-5.
- 660 24. Ben-Nejma, I.R.H., et al., *Increased soluble amyloid-beta causes early aberrant brain network*  
661 *hypersynchronisation in a mature-onset mouse model of amyloidosis.* Acta Neuropathol  
662 Commun, 2019. **7**(1): p. 180.
- 663 25. Berger, Z., et al., *Accumulation of pathological tau species and memory loss in a conditional*  
664 *model of tauopathy.* J Neurosci, 2007. **27**(14): p. 3650-62.
- 665 26. Kopeikina, K.J., et al., *Tau accumulation causes mitochondrial distribution deficits in neurons*  
666 *in a mouse model of tauopathy and in human Alzheimer's disease brain.* Am J Pathol, 2011.  
667 **179**(4): p. 2071-82.
- 668 27. Koss, D.J., et al., *Mutant Tau knock-in mice display frontotemporal dementia relevant*  
669 *behaviour and histopathology.* Neurobiol Dis, 2016. **91**: p. 105-23.
- 670 28. Jin, M., et al., *Soluble amyloid beta-protein dimers isolated from Alzheimer cortex directly*  
671 *induce Tau hyperphosphorylation and neuritic degeneration.* Proc Natl Acad Sci U S A, 2011.  
672 **108**(14): p. 5819-24.
- 673 29. Ciccone, R., et al., *Amyloid  $\beta$ -Induced Upregulation of Na(v)1.6 Underlies Neuronal*  
674 *Hyperactivity in Tg2576 Alzheimer's Disease Mouse Model.* Sci Rep, 2019. **9**(1): p. 13592.
- 675 30. Selkoe, D.J. and J. Hardy, *The amyloid hypothesis of Alzheimer's disease at 25 years.* EMBO  
676 Mol Med, 2016. **8**(6): p. 595-608.
- 677 31. Beckman, D., et al., *Oligomeric A $\beta$  in the monkey brain impacts synaptic integrity and induces*  
678 *accelerated cortical aging.* Proc Natl Acad Sci U S A, 2019. **116**(52): p. 26239-26246.
- 679 32. Baerends, E., et al., *Modeling the early stages of Alzheimer's disease by administering*  
680 *intracerebroventricular injections of human native A $\beta$  oligomers to rats.* Acta Neuropathol  
681 Commun, 2022. **10**(1): p. 113.
- 682 33. Bolmont, T., et al., *Induction of tau pathology by intracerebral infusion of amyloid-beta -*  
683 *containing brain extract and by amyloid-beta deposition in APP x Tau transgenic mice.* Am J  
684 Pathol, 2007. **171**(6): p. 2012-20.
- 685 34. Aoki, M., et al., *Amyloid beta-peptide levels in laser capture microdissected cornu ammonis 1*  
686 *pyramidal neurons of Alzheimer's brain.* Neuroreport, 2008. **19**(11): p. 1085-9.
- 687 35. Perdigão, C., et al., *Intracellular Trafficking Mechanisms of Synaptic Dysfunction in*  
688 *Alzheimer's Disease.* Front Cell Neurosci, 2020. **14**: p. 72.
- 689 36. Umeda, T., et al., *Intraneuronal amyloid  $\beta$  oligomers cause cell death via endoplasmic*  
690 *reticulum stress, endosomal/lysosomal leakage, and mitochondrial dysfunction in vivo.* J  
691 Neurosci Res, 2011. **89**(7): p. 1031-42.
- 692 37. Nishitsuji, K., et al., *The E693Delta mutation in amyloid precursor protein increases*  
693 *intracellular accumulation of amyloid beta oligomers and causes endoplasmic reticulum*  
694 *stress-induced apoptosis in cultured cells.* Am J Pathol, 2009. **174**(3): p. 957-69.
- 695 38. Montine, T.J., et al., *National Institute on Aging-Alzheimer's Association guidelines for the*  
696 *neuropathologic assessment of Alzheimer's disease: a practical approach.* Acta Neuropathol,  
697 2012. **123**(1): p. 1-11.
- 698 39. Braak, H., et al., *Staging of Alzheimer disease-associated neurofibrillary pathology using*  
699 *paraffin sections and immunocytochemistry.* Acta Neuropathol, 2006. **112**(4): p. 389-404.
- 700 40. Hyman, B.T., et al., *National Institute on Aging-Alzheimer's Association guidelines for the*  
701 *neuropathologic assessment of Alzheimer's disease.* Alzheimers Dement, 2012. **8**(1): p. 1-13.
- 702 41. Braak, H., et al., *Staging of brain pathology related to sporadic Parkinson's disease.*  
703 Neurobiol Aging, 2003. **24**(2): p. 197-211.
- 704 42. McKeith, I.G., et al., *Diagnosis and management of dementia with Lewy bodies: Fourth*  
705 *consensus report of the DLB Consortium.* Neurology, 2017. **89**(1): p. 88-100.

- 706 43. McKeith, I.G., et al., *Diagnosis and management of dementia with Lewy bodies: third report*  
707 *of the DLB Consortium*. *Neurology*, 2005. **65**(12): p. 1863-72.
- 708 44. Walker, L., et al., *Quantitative neuropathology: an update on automated methodologies and*  
709 *implications for large scale cohorts*. *J Neural Transm (Vienna)*, 2017. **124**(6): p. 671-683.
- 710 45. Iulita, M.F., et al., *Intracellular A $\beta$  pathology and early cognitive impairments in a transgenic*  
711 *rat overexpressing human amyloid precursor protein: a multidimensional study*. *Acta*  
712 *Neuropathol Commun*, 2014. **2**: p. 61.
- 713 46. Youmans, K.L., et al., *Intraneuronal A $\beta$  detection in 5xFAD mice by a new A $\beta$ -specific*  
714 *antibody*. *Mol Neurodegener*, 2012. **7**: p. 8.
- 715 47. Arriagada, P.V., et al., *Neurofibrillary tangles but not senile plaques parallel duration and*  
716 *severity of Alzheimer's disease*. *Neurology*, 1992. **42**(3 Pt 1): p. 631-9.
- 717 48. Guillozet, A.L., et al., *Neurofibrillary tangles, amyloid, and memory in aging and mild*  
718 *cognitive impairment*. *Arch Neurol*, 2003. **60**(5): p. 729-36.
- 719 49. Collins-Praino, L.E., et al., *Soluble amyloid beta levels are elevated in the white matter of*  
720 *Alzheimer's patients, independent of cortical plaque severity*. *Acta Neuropathol Commun*,  
721 2014. **2**: p. 83.
- 722 50. Wu, R., et al., *Seeding-Competent Tau in Gray Matter Versus White Matter of Alzheimer's*  
723 *Disease Brain*. *J Alzheimers Dis*, 2021. **79**(4): p. 1647-1659.
- 724 51. Zheng, W.H., et al., *Amyloid beta peptide induces tau phosphorylation and loss of cholinergic*  
725 *neurons in rat primary septal cultures*. *Neuroscience*, 2002. **115**(1): p. 201-11.
- 726 52. De Felice, F.G., et al., *Alzheimer's disease-type neuronal tau hyperphosphorylation induced*  
727 *by A beta oligomers*. *Neurobiol Aging*, 2008. **29**(9): p. 1334-47.
- 728 53. Ma, Q.L., et al., *Antibodies against beta-amyloid reduce Abeta oligomers, glycogen synthase*  
729 *kinase-3beta activation and tau phosphorylation in vivo and in vitro*. *J Neurosci Res*, 2006.  
730 **83**(3): p. 374-84.
- 731 54. Zhang, H.Y., et al., *Reduction of amyloid beta by A $\beta$ 3-10-KLH vaccine also decreases tau*  
732 *pathology in 3xTg-AD mice*. *Brain Res Bull*, 2018. **142**: p. 233-240.
- 733 55. Blennow, K., et al., *Effect of immunotherapy with bapineuzumab on cerebrospinal fluid*  
734 *biomarker levels in patients with mild to moderate Alzheimer disease*. *Arch Neurol*, 2012.  
735 **69**(8): p. 1002-10.
- 736 56. Lehmann, S., et al., *Cerebrospinal fluid A beta 1-40 peptides increase in Alzheimer's disease*  
737 *and are highly correlated with phospho-tau in control individuals*. *Alzheimers Res Ther*, 2020.  
738 **12**(1): p. 123.
- 739 57. Koo, E.H. and S.L. Squazzo, *Evidence that production and release of amyloid beta-protein*  
740 *involves the endocytic pathway*. *J Biol Chem*, 1994. **269**(26): p. 17386-9.
- 741 58. Fourriere, L. and P.A. Gleeson, *Amyloid  $\beta$  production along the neuronal secretory pathway:*  
742 *Dangerous liaisons in the Golgi?* *Traffic*, 2021. **22**(9): p. 319-327.
- 743 59. Tam, J.H., C. Seah, and S.H. Pasternak, *The Amyloid Precursor Protein is rapidly transported*  
744 *from the Golgi apparatus to the lysosome and where it is processed into beta-amyloid*. *Mol*  
745 *Brain*, 2014. **7**: p. 54.
- 746 60. Brewer, G.J., et al., *Age-Related Intraneuronal Aggregation of Amyloid- $\beta$  in Endosomes,*  
747 *Mitochondria, Autophagosomes, and Lysosomes*. *J Alzheimers Dis*, 2020. **73**(1): p. 229-246.
- 748 61. Koss, D.J., et al., *RAB39B is redistributed in dementia with Lewy bodies and is sequestered*  
749 *within a $\beta$  plaques and Lewy bodies*. *Brain Pathol*, 2020.
- 750 62. Jordan, K.L., et al., *Therapeutic Targeting of Rab GTPases: Relevance for Alzheimer's Disease*.  
751 *Biomedicines*, 2022. **10**(5).
- 752 63. Lai, A.Y. and J. McLaurin, *Mechanisms of amyloid-Beta Peptide uptake by neurons: the role of*  
753 *lipid rafts and lipid raft-associated proteins*. *Int J Alzheimers Dis*, 2010. **2011**: p. 548380.
- 754 64. Welikovitch, L.A., et al., *Evidence of intraneuronal A $\beta$  accumulation preceding tau pathology*  
755 *in the entorhinal cortex*. *Acta Neuropathol*, 2018. **136**(6): p. 901-917.

- 756 65. Gouras, G.K., et al., *Intraneuronal Abeta42 accumulation in human brain*. Am J Pathol, 2000.  
757 **156**(1): p. 15-20.
- 758 66. Wirths, O., et al., *Intraneuronal Abeta accumulation precedes plaque formation in beta-*  
759 *amyloid precursor protein and presenilin-1 double-transgenic mice*. Neurosci Lett, 2001.  
760 **306**(1-2): p. 116-20.
- 761 67. Wegiel, J., et al., *Intraneuronal Abeta immunoreactivity is not a predictor of brain*  
762 *amyloidosis-beta or neurofibrillary degeneration*. Acta Neuropathol, 2007. **113**(4): p. 389-  
763 402.
- 764 68. Oddo, S., et al., *A dynamic relationship between intracellular and extracellular pools of*  
765 *Abeta*. Am J Pathol, 2006. **168**(1): p. 184-94.
- 766 69. Mori, C., et al., *Intraneuronal Abeta42 accumulation in Down syndrome brain*. Amyloid,  
767 2002. **9**(2): p. 88-102.
- 768 70. Umeda, T., et al., *Intracellular amyloid  $\beta$  oligomers impair organelle transport and induce*  
769 *dendritic spine loss in primary neurons*. Acta Neuropathol Commun, 2015. **3**: p. 51.
- 770 71. Silvestro, S., A. Valeri, and E. Mazzon, *Aducanumab and Its Effects on Tau Pathology: Is This*  
771 *the Turning Point of Amyloid Hypothesis?* Int J Mol Sci, 2022. **23**(4).
- 772 72. Clavaguera, F., et al., *Transmission and spreading of tauopathy in transgenic mouse brain*.  
773 Nat Cell Biol, 2009. **11**(7): p. 909-13.
- 774 73. Iba, M., et al., *Synthetic tau fibrils mediate transmission of neurofibrillary tangles in a*  
775 *transgenic mouse model of Alzheimer's-like tauopathy*. J Neurosci, 2013. **33**(3): p. 1024-37.
- 776 74. Guo, J.L., et al., *Unique pathological tau conformers from Alzheimer's brains transmit tau*  
777 *pathology in nontransgenic mice*. J Exp Med, 2016. **213**(12): p. 2635-2654.

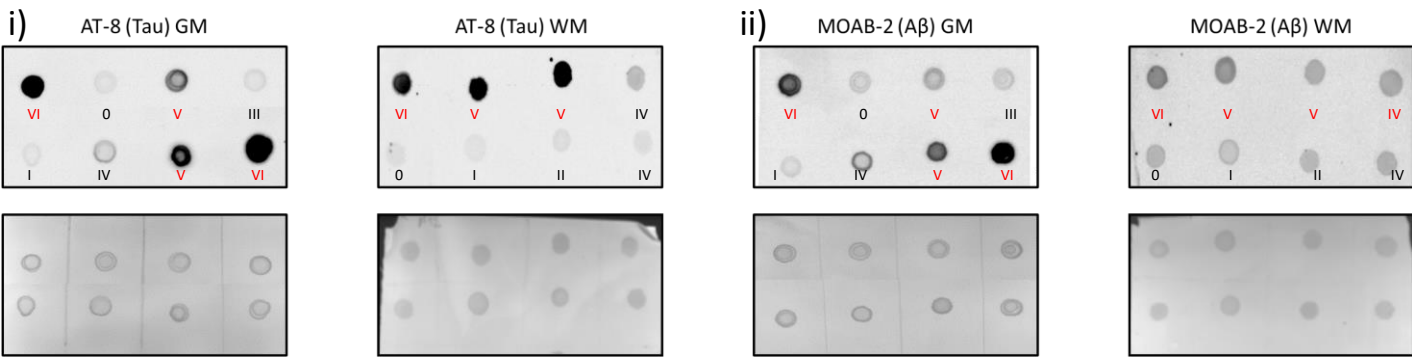
778



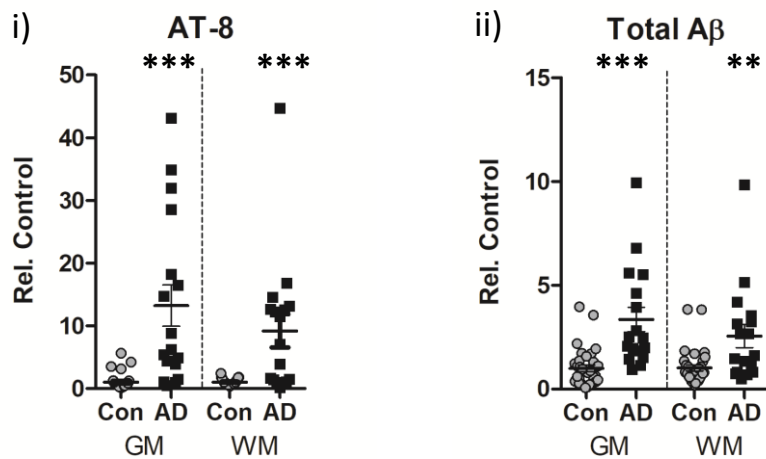
Disease	N	Sex (% Male)	Age (years)	PMI (hrs)	NFT Braak stage	Thal Phase	CERAD	NIA-AA	LB Braak stage	McKeith Criteria
Immuno-blot										
Con	35	57.1%	47-97 80.5±2.2	16-95 45.8±3.7	0-IV 17.1% -0 17.1% - I 25.7% - II 25.7% -III 14.3% -VI	0-4 20%-0 22.9%-1 25.7%-2 22.9%-3 8.6%-4	0-2 80%-0 5.7%-1 14.3%-2	0-2 20% - 0 65.7% - 1 14.3% - 2	0-3 91.4%-0 2.9%-1 5.7%-3	91.4%-No LB 8.6%-Brainstem
AD	17	35.3%	74-96 85.5±1.5	5-90 57.2±5.7	V-VI 29.4% -V 70.6% -VI	4-5 15.4%-4 84.6%-5	3 100% -3	3 100% - 3	0-3 82.3%-0 11.8%-2 5.9%-3	76.5% -No LB 17.6% -Brainstem 5.9%-Limbic
Immunohistochemistry (AT-8 and 48G plaques)										
Con	36	56.2%	55-97 81.5±2.2	16-95 47.8 ±3.9	0-IV 16.7% -0 19.4%- I 25% - II 25%-III 13.9%-VI	0-4 16.7%-0 25%-1 30.6%-2 19.4%-3 8.3%-4	0-2 77.8%-0 8.3%-1 13.9%-2	0-2 16.7%-0 69.4%-1 13.9%-2	0-3 88.1%-0 5.8%-1 6.1%-3	88.7%-No LB 8.3%-Brainstem 2.8%-Limbic
AD	20	30%	70-93 85±1.3	5-90 54.4±4.9	V-VI 25%-V 75%-VI	4-5 13.9%-4 86.1%-5	3 100%-3	3 100%-3	0-3 85%-0 10%-2 5%-3	80% -No LB 15%-Brainstem 5%-Limbic
Immunohistochemistry (AT-8 and MOAB-2 intracellular Aβ)										
Con	14	28.6%	70-97 85.6±2.4	16-95 45.1 ±7.3	0-IV 7.1% -0 14.3%- I 42.9% - II 35.7%-III	0-2 28.6%-0 35.7%-1 35.7%-2	0-1 85.7%-0 14.3%-1	0-1 35.7%-0 64.3%-1	0-3 85.7%-0 14.3%-3	78.6%-No LB 14.3%-Brainstem 7.1%-Limbic
AD	8	12.5%	78-93 85.4±1.8	29-90 57±7.5	V-VI 12.5%-V 87.5%-VI	4-5 12.5%-4 87.5%-5	3 100%-3	3 100%-3	0-3 87.5%-0 12.5%-2	75% -No LB 25%-Brainstem

**Table 1. Human tissue cohort.** Human cases using in tissue microarray and western blot separated by disease classification according to non-diseased controls (Con), Alzheimer's disease (AD) and dementia with Lewy bodies (DLB). Case numbers (n), sex, age, post-mortem interval (PMI), neurofibrillary tangle (NFT) Braak stage, Thal phase, Consortium to Establish a Registry for Alzheimer's Disease (CERAD), the National Institute of Ageing – Alzheimer's Association (NIA-AA) criteria, Lewy body (LB) Braak stage and McKeith criteria are provided. For age and PMI both range and mean  $\pm$ SEM are provided. For numerical scores of pathology, range and percentage composition are given. For McKeith criteria, only percentage composition is given, where cases free of LBs (No LB), amygdala predominate (Amyg), limbic predominate (Limb) and neocortical predominate (Neo) are indicated. \* indicates composition based on available data.

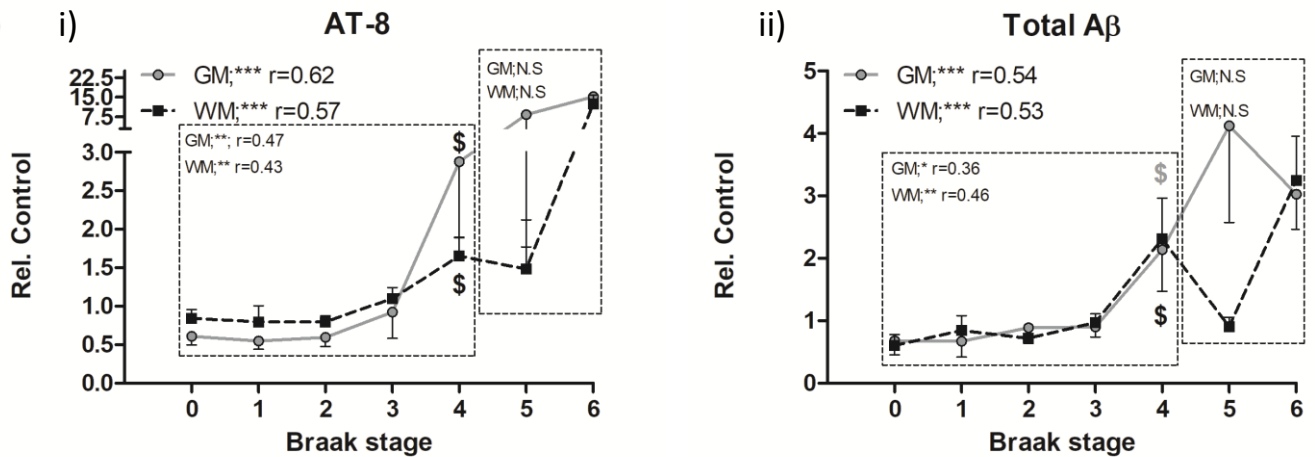
A)



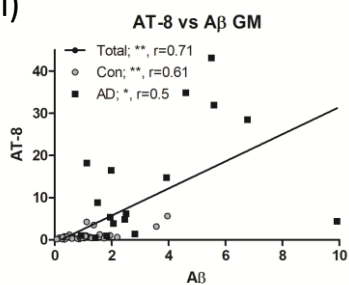
B)



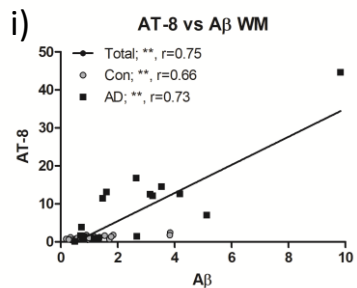
C)



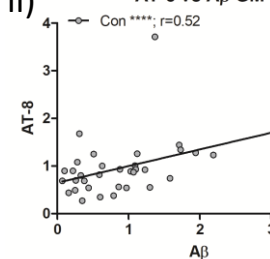
D) i)



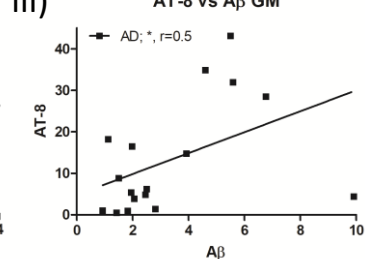
e) i)



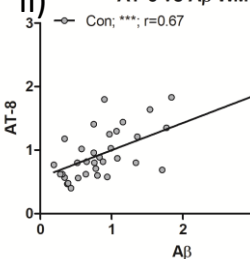
ii) **AT-8 vs A $\beta$  GM**



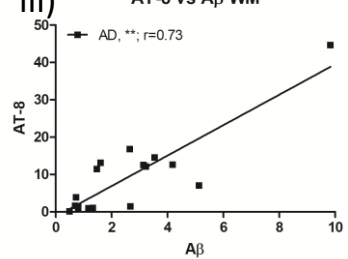
iii) **AT-8 vs A $\beta$  GM**



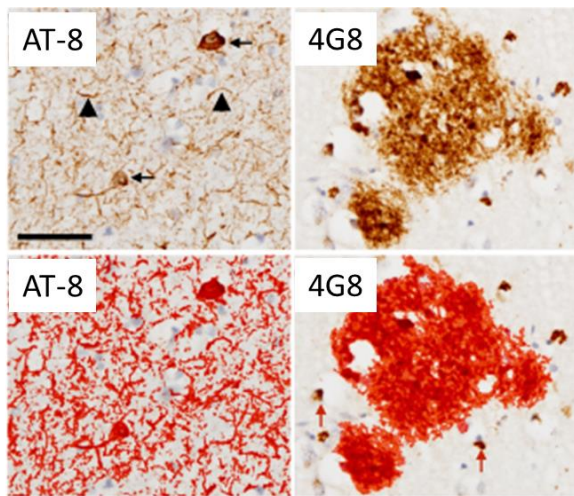
ii) **AT-8 vs A $\beta$  WM**



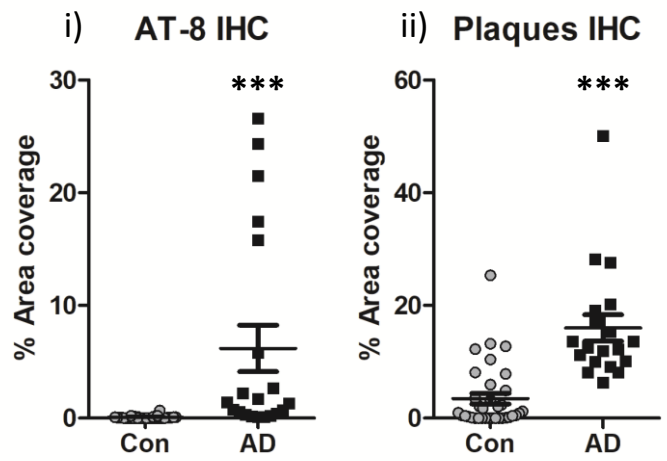
iii) **AT-8 vs A $\beta$  WM**



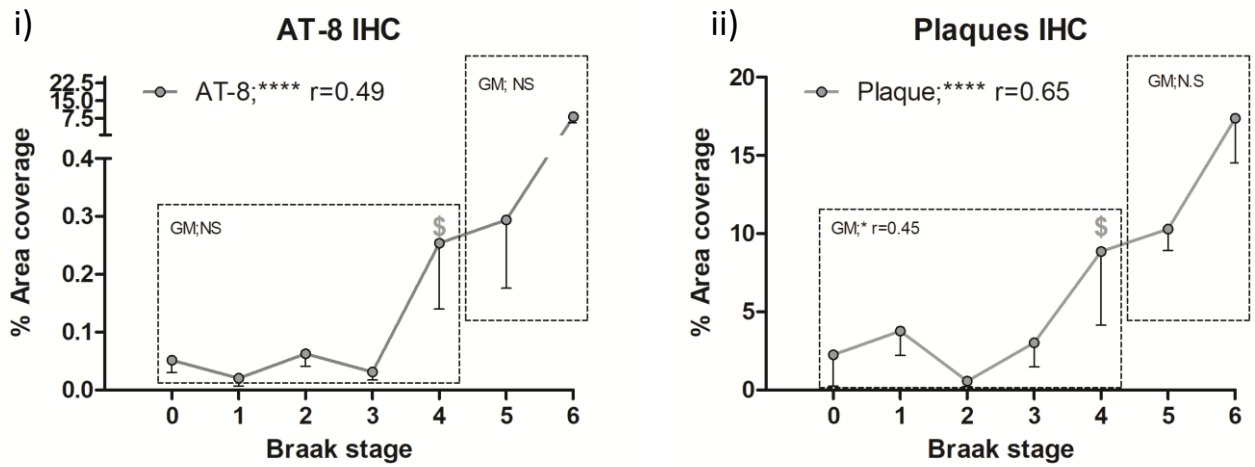
A)



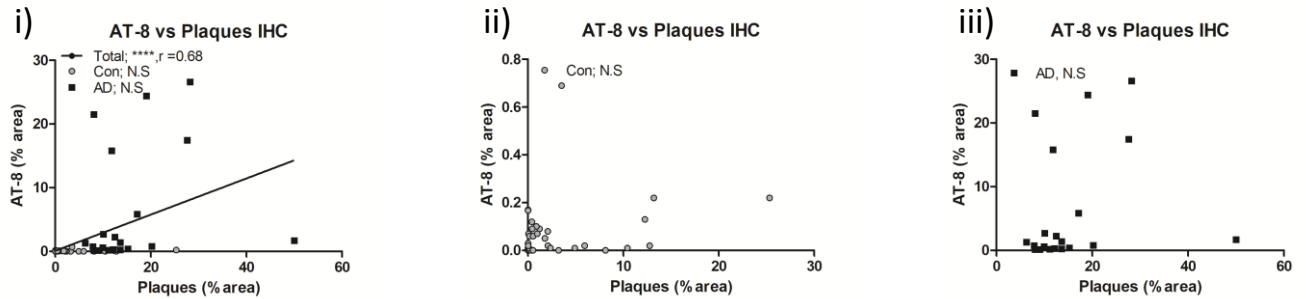
B)

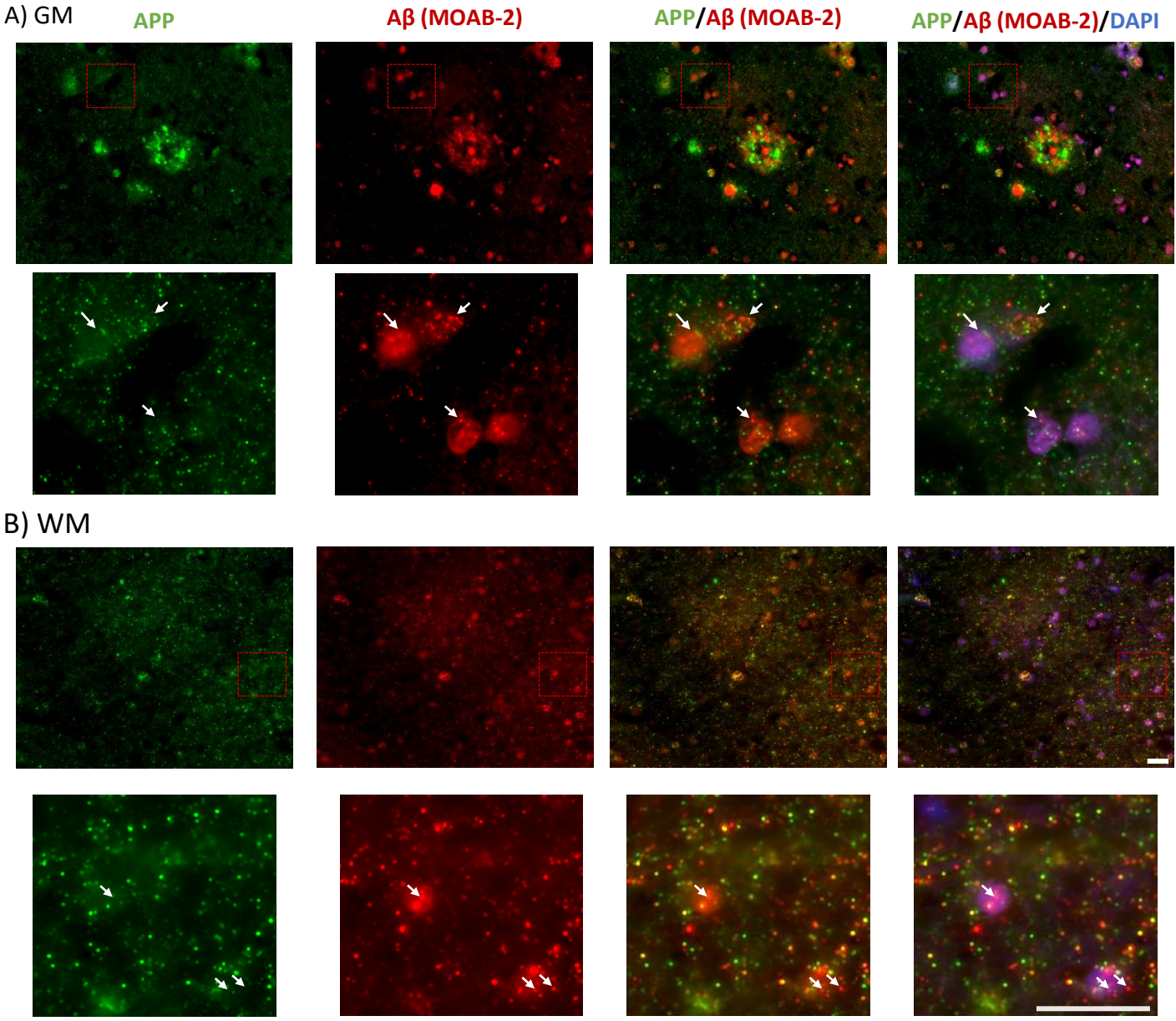


C)



D)





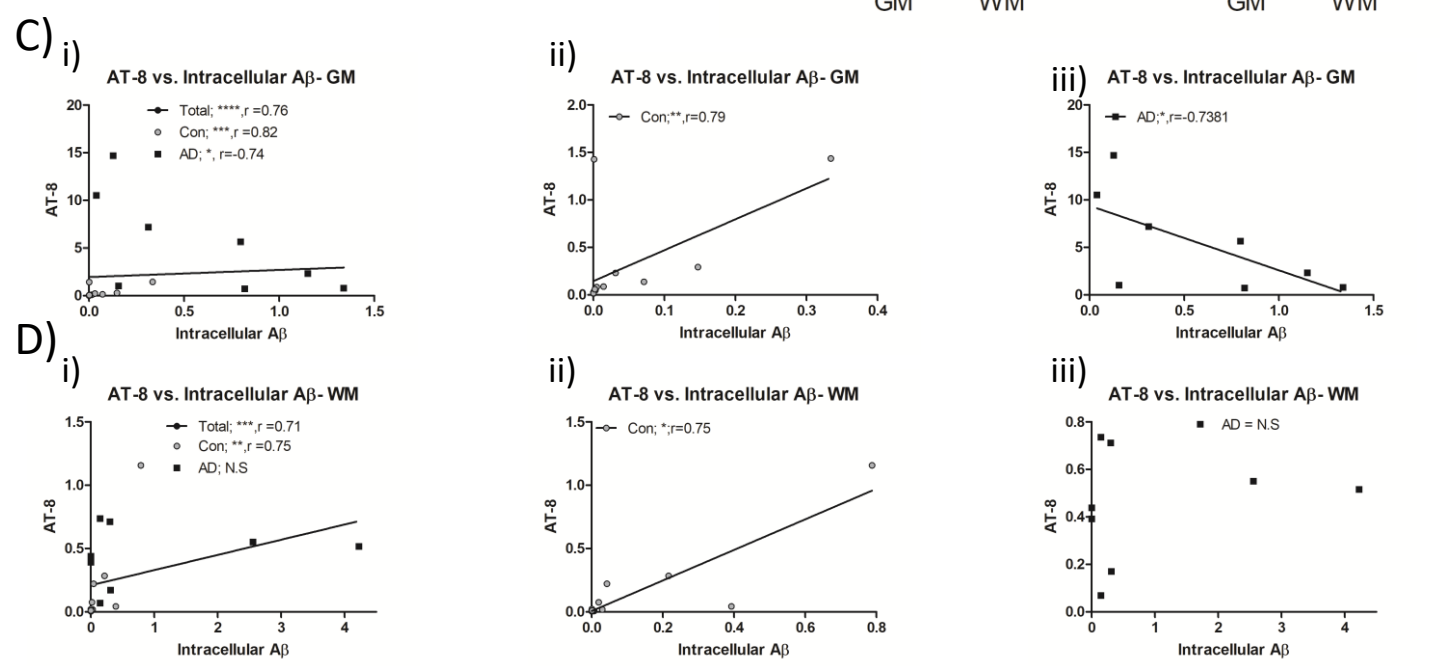
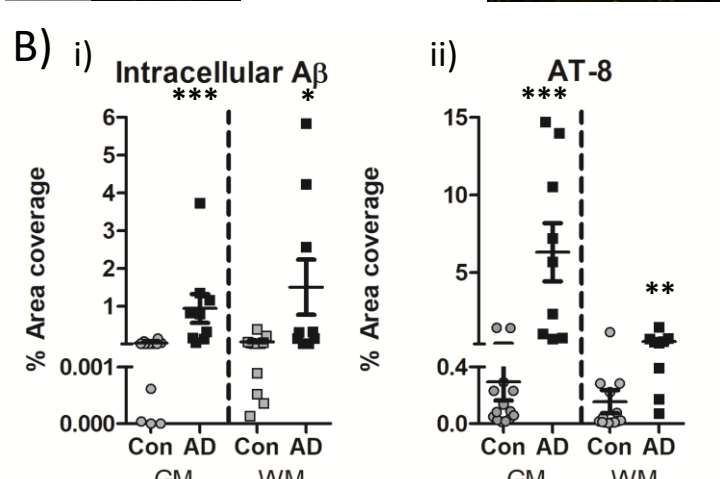
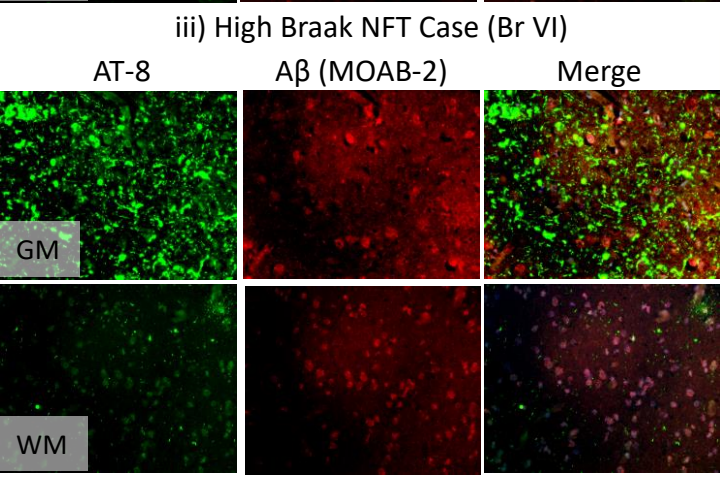
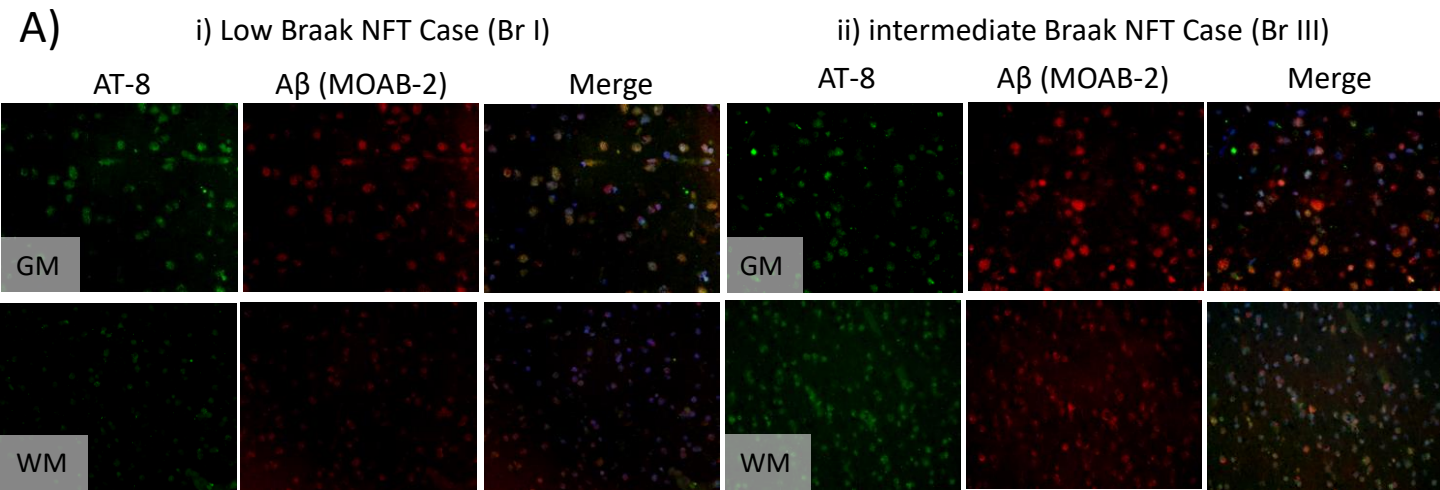


Figure 5

